Journal of Cellular Biochemistry 98:966–980 (2006)

Innate Immune Response to Human Bone Marrow Fibroblastic Cell Implantation in CB17 Scid/Beige Mice

Zhidao Xia,[1,3] Philip R. Taylor,[2] Rachel M. Locklin,[1] Siamon Gordon,[2] Zhanfeng Cui,[3] and James T. Triffitt[1]*

[1]Botnar Research Centre, Institute of Musculoskeletal Science, Nuffield Department of Orthopaedic Surgery, The University of Oxford, Oxford, OX3 7LD, United Kingdom
[2]Sir William Dunn School of Pathology, the University of Oxford, Oxford, United Kingdom
[3]Department of Engineering Science, the University of Oxford, Oxford, United Kingdom

Abstract Immunocompromised mouse models have been extensively used to assess human cell implantation for evaluation of cytotherapy, gene therapy and tissue engineering strategies, as these mice are deficient in T and B lymphoid cells. However, the innate immune response and its effect on human cell xenotransplantation in these mouse models are mainly unknown. The aim of this study is to characterise the myeloid populations in the spleen and blood of CB17 scid beige (CB17 sb) mice, and to study the inflammatory cell responses to xenogeneic implantation of enhanced green fluorescent protein (GFP)-labelled human bone marrow fibroblastic (HBMF) cells into CB17 sb mice. The results indicate that even though CB17 sb mice are deficient in B- and T-cells, they exhibit some increases in their monocyte (Mo), macrophage (MΦ) and neutrophil (Neu) populations. NK cell and eosinophil populations show no differences compared with wild-type Balb/C mice. An innate immune response, identified by CR3 (CD11b/CD18)-positive myeloid inflammatory cells and F4/80-positive macrophages, was evident in the tissues where HBMF cells were implanted. As a consequence, the majority of implanted HBMF cells were eliminated by 4 weeks after implantation. Interestingly, the mineralised matrix formed by osteogenic HBMF cells was also eroded by multinuclear MΦ-like giant cells. We conclude that CB17 sb mice retain active innate immune cells, which respond to HBMF cell xenotransplantation. This study highlights the importance of the innate immune cells in the anti-xenograft response and suggests that strategies to block the activities of these cells may ameliorate the progressive long-term elimination of xenotransplants. J. Cell. Biochem. 98: 966–980, 2006.

Key words: innate immune response; human bone marrow fibroblastic (HBMF) cells; macrophages; xenotransplantation; green fluorescent protein (GFP); CB17 scid beige mice

Human bone marrow fibroblastic (HBMF) cells or mesenchymal stem cells (MSCs) are a nonhaematopoietic adherent cell population that can be isolated by direct cultivation of whole bone marrow cells [Pittenger et al., 1999]. This cell population and its osteogenic potential were first identified by Friedenstein in the early 70s [Friedenstein et al., 1970]. Owen [1988] introduced the concept of the stromal cell system, in which bone marrow fibroblastic cells, such as those that reside within the marrow, maintain a level of self-renewal, and give rise to cells that can differentiate into various connective tissue lineages. Suggestions have been given to design cell therapies for the reconstruction of mesenchymal tissues, including bone, cartilage, muscle, marrow stroma, tendon, fat, dermis and connective tissues using MSCs [Caplan, 1994]. Recently, MSCs have

Abbreviations used: Mo, monocytes; MΦ, macrophages; MnGC, multinuclear giant cells; human bone marrow fibroblastic (HBMF) cells; CB17 sb, CB17 scid/beige mouse.

This article contains supplementary material, which may be viewed at the Journal of Cellular Biochemistry website at http://www.interscience.wiley.com/jpages/0730-2312/suppmat/index.html.

Grant sponsor: Wellcome Trust, the Medical Research Council and the Arthritis Research Campaign, UK.

*Correspondence to: James T. Triffitt, Botnar Research Centre, Institute of Musculoskeletal Science, Nuffield Department of Orthopaedic Surgery, The University of Oxford, Oxford, OX3 7LD, UK.
E-mail: james.triffitt@ndos.ox.ac.uk

Received 28 June 2005; Accepted 18 October 2005
DOI 10.1002/jcb.20730

been studied extensively in terms of their identification, differentiation and distribution [Liechty et al., 2000; Triffitt et al., 2001; Niyibizi et al., 2004]. In particular, their potential for bone formation and their use in bone tissue engineering, gene therapy [Tsuda et al., 2003] and clinical applications are under active investigation.

It is currently widely accepted that for cell therapy autogenous MSCs are preferable. However, allogeneic MSCs are also applied systemically in vivo [Lee et al., 2003]. Adult MSCs have been suggested to decrease lymphocyte proliferation in vitro [Gotherstrom et al., 2003] and may even have a potent immunosuppressive effect in vivo [Le Blanc et al., 2004]. Thus this phenomenon suggests MSCs may have potentially wide clinical applications. Allografts in experimental animals have been used to reconstruct bone defects without the use of immunosuppressive therapy [Arinzeh et al., 2003]. However, marrow stromal progenitors reinfused in patients receiving a T-cell-depleted allograft have a limited capacity to reconstitute marrow mesenchymal cells [Cilloni et al., 2000]. It has been found that MSCs isolated from recipients of allogeneic transplantation are not of donor genotype despite successful donor type haematopoietic engraftment [Koc et al., 1999]. Whether this is due to an unsuitable environment or to host immune responses to MSCs and related therapies is unknown.

In order to obtain reliable models to evaluate MSC therapies, immunocompromised mice, such as CB17 scid beige or severe combined immunodeficient (SCID) mice have been used extensively. SCID background mice are used to host human cells and provide valuable tools to investigate their potential for human cell therapy, gene therapy and tissue engineering applications [Lee et al., 2001; Gronthos et al., 2003]. This is because SCID background mice lack functional T- and B-cells as a result of a defective recombinase system necessary for rearrangement of antigen-specific receptors [Schuler et al., 1986].

It has been proposed that mesenchymal stem cells have unique immunologic characteristics that allow persistence in a xenogeneic environment [Liechty et al., 2000]. However, the survival of human cells, in particular human bone marrow fibroblastic (HBMF) cells, in immunocompromised mice remains limited and only persists short-term [Toma et al., 2002]. By systematic delivery of retroviral transfected HBMF cells encoding human interleukin 3 (hIL3) in vivo into NOD/SCID mice, it has been shown that the peak of hIL-3 expression demonstrated in host serum is at 1 week then decreases over time [Lee et al., 2001]. Pretreatment of SCID mice with radiation before xenotransplantation of human bone and subsequent administration of anti-asialo GM1 antiserum every 7 days to deplete mouse macrophage and natural killer (NK) cell activity led to xenogeneic human bone survival with new bone formation [Boynton et al., 1996]. This implies that the innate immune system, consisting predominantly of polymorphonuclear leukocytes, monocytes (Mo)/macrophages (MΦ) and NK cells, may be responsible for elimination of human cell implants in immunocompromised mice [Fox et al., 2001].

Our previous work indicated that encouraging stem and progenitor cells to progress towards osteogenesis by prolonged dexamethasone treatment resulted in the greatest bone formation within diffusion chambers (DCs) or scaffolds [Gundle et al., 1995]. However, direct grafts of human cells alone into immunocompromised or cortisone-treated animals has also been used with some success to assess the developmental capability of the grafted cells [Yamamoto et al., 1991]. In the present studies it was considered that, (a) to encourage any continuation of the bone tissue formation induced by osteogenic culture following implantation in vivo and (b) to assess the potential for any remaining immune cell responses to the human products alone, the most appropriate scaffold to induce further development was the extracellular matrix produced by the cells themselves in similar confluent layers. Furthermore, freshly scraped mouse marrow stromal cell lines directly inoculated subcutaneously into nude mice have been shown to exhibit osteogenic activity and after 4 weeks appreciable bone tissue can be observed [Matsumoto et al., 2005].

Xenografts, like allografts, are presumed to elicit cell-mediated immune responses resulting in chronic rejection [Platt, 1999]. Antibody-dependent adaptive immune responses to xenografts are dominated by B- and T-lymphocytes and their clinical significance has been investigated extensively. In contrast, relatively little attention has been paid to the pro-inflammatory role of innate immunity on donor

cell survival and differentiation [Fox and Harrison, 2000].

CB17 SCID/beige (CB17 sb) mice are derived from CB17 scid (no T- and B-cells) and B6 bg mice (no NK activity) and are doubly homozygous for scid and beige (bg) [Froidevaux and Loor, 1991]. Mice with both of these immunodeficiencies should be better recipients for xenografts than classical scid mice [Froidevaux and Loor, 1991]. Lacking B- and T-cells as well as having a defect in NK cell activity makes the CB17 sb mouse strain an ideal model for the study of host innate immune responses to implanted HBMF cells and the effects of this on donor cell survival, differentiation potential and function. Previous experiments in our laboratory have shown that implantation of HBMF cells and/or polymer materials in non-obese diabetic/severe combined immunodeficient (NOD/SCID) mice induced recruitment of neutrophils, monocytes, macrophages, generation of foreign body giant cells and mast cell infiltration for up to 8 weeks in vivo [Xia et al., 2004]. However, little is known about the remaining host innate immune responses to HBMF cells in CB17 sb mice. Recently, a rapid ex vivo identification of myeloid cells has been developed that makes it possible to analyse the characteristics of monocytes/macrophages, neutrophils, eosinophils and natural killer (NK) cells [Taylor et al., 2003]. The aim of the current study was to characterise the populations of innate immune cells in spleen and blood and their distribution in tissues after xenogeneic implantation of HBMF cells into CB17 bg mice. The potential role of macrophages in elimination of HBMF cells and their mineralised matrix is also investigated. As reported, CB17 sb mice are deficient in T- and B-cells, but they have normal or increased numbers of neutrophils, Mo and MΦ compared with wild-type Balb\C mice. Mo/MΦ as well as CR3-positive cells infiltrate tissue sites containing HBMF cells. We have also observed F4/80 (a marker of macrophages) and CR3 (the receptor for the complement component, CR3/CD11b) positive cells eroding ectopic mineralised matrix formed by implanted HBMF cells.

MATERIALS AND METHODS

Cell Culture and Retroviral Transfection

Primary human bone marrow fibroblastic (HBMF) cell cultures were prepared as described previously [Oreffo et al., 1999]. In brief, trabecular bone samples were obtained from haematologically normal patients undergoing routine total hip replacement surgery. Only tissue that would have been discarded was used, with the approval of the local hospital management committee. Trabecular bone containing bone marrow was gently crushed in αMEM (Gibco BRL, Invitrogen Ltd., Paisley, UK), the tissue repeatedly vortexed (Vortex-GENIE. K-550-GE, Scientific Industries, Inc., UK) and the resultant cell suspension filtered through a 70 μm cell strainer (Falcon, Fahrenheit, Milton Keynes, UK) to obtain a single-cell suspension. Cells were then centrifuged and resuspended in αMEM before seeding at a density of $1–2 \times 10^5$ cells/cm^2 for culture in 10% fetal calf serum (FCS) αMEM.

Primary HBMF cells were transduced using a modified retroviral pseudotype of the murine leukemia virus, MuLV 4073, containing a retroviral vector encoding enhanced green fluorescent protein (eGFP) and *Neo*^{r} genes (kindly supplied by Oxford Biomedica Plc., Oxford, UK). Concentrated MuLV 4073 were diluted 1:200 in 20% FCS αMEM containing 4 μg/ml polybrene (Sigma, Sigma-Aldrich Company Ltd., Dorset, UK) to transduce HBMF cells 6 h/day for 3 days. Culture medium containing retroviral vectors was replaced by normal culture medium (10% FCS in αMEM) after each of the three viral transductions [Xia et al., 2005].

In the experiments described, the cells were used after two to four passages. All culture medium contained penicillin 100 U/ml and streptomycin 100 μg/ml (final concentrations), and cultures were maintained at 37°C in a humidified atmosphere of 5% CO_2 in air in a commercial incubator.

Animal Model and In Vivo Implantation of HBMF Cells

All mice used in this study were between 6 and 10 weeks of age. Balb/C and CB17 scid beige mice were purchased from the Biomedical Services, University of Oxford. Animals were maintained and handled in accordance with strict institutional and UK Home Office guidelines.

To screen for innate immune cell markers, three Balb/C mice were used as wild-type controls. CB17 scid beige mice, three controls and six obtained after HBMF cell implantation were used for FACS analysis of blood and spleen and immunohistochemistry of spleen and tibia.

For implantation, GFP-labelled HBMF cells were cultured in αMEM containing 10% FCS for up to 7 days to allow cell proliferation to confluence, before the culture medium was switched to osteogenic medium, consisting of 10% FCS in αMEM with supplements of 10^{-8} M dexamethasone and 100 μM L-ascorbic acid-2-phosphate to induce osteogenic differentiation. Cultures were continued for 10 days and media replaced every 3–5 days. After matrix formation was observed by light microscopy, the cells were washed twice in PBS, and the cell sheets detached with a disposable cell scraper. The cell sheet was collected in a centrifuge tube, centrifuged at 250*g* and resuspended in ice cold PBS. The estimated cell number per T175 culture flask was 2×10^6 as determined by cell counting. Thirty-six CB17 sb mice were randomly divided into two groups and under general anaesthesia the anterior tibialis muscle was surgically separated from the tibial surface. In the treatment group, a pellet of HBMF (1×10^6) cells was implanted between the tibia and the anterior tibialis muscle. Sham operated mice served as controls without cell implantation. One, 2 and 4 weeks post-operatively, six mice in each group were killed and tissue samples were either immediately embedded in Cryo-M-bed, (Bright Instrument Company Ltd., UK) on dry ice for cryosectioning, or frozen in liquid nitrogen and stored at −80°C for isolation of total RNA for RT-PCR analysis.

FACS Analysis

Splenocytes were harvested by standard methods using a combination of digestion with "Liberase Blendzyme II" in RPMI (Roche Molecular Biochemicals, East Sussex, UK) and mechanical dissociation [Taylor et al., 2003]. Enzyme activity was quenched with RPMI: 20% FCS, erythrocytes lysed with Gey's hypotonic solution and cell debris removed by centrifugation through 100% FCS at 300*g*.

Peripheral blood was collected by exanguination by cardiac puncture following cervical dislocation into 0.1 volume of 100 mM EDTA, pH 8.0. Cells were harvested by centrifugation and resuspended in 50 volumes of Gey's solution to lyse erythrocytes. Peripheral blood leukocytes were then recovered by centrifugation through FCS as described above.

FACS analysis of surface antigen expression was performed according to conventional protocols at 4°C in the presence of 2 mM NaN_3. Cells were blocked with 5% heat-inactivated rabbit serum; 0.5% BSA; 5 mM EDTA, and 10 μg/ml 2.4 G2 (anti-FcγRII and III) prior to the addition of primary antibodies. Biotinylated antibodies were detected using streptavidin–allophycocyanin (BD Pharmingen, Oxford, UK). Cells were fixed with 1% formaldehyde in PBS prior to analysis on a BD FACScalibur with Cell Quest software.

The following antibodies (Table I) were used in this study: F4/80-PE (Serotec), Gr-1-PE (anti-Ly6C/G; BD Pharmingen), 5C6-FITC (Serotec; anti-CR3/CD11b), CD3, B220, CD49b, 2A11 (Serotec; anti-Dectin-1) and isotype matched control antibodies.

Histochemistry, Immunohistochemistry, Histomorphometry and Microscopy

The frozen undecalcified tissue samples were cryosectioned (Reichert-Jung Cryostat 2800, Cambridge Instruments Ltd., Cambridge, UK) and mounted on glass slides. After air drying the sections were stored at −20°C before staining. Tartrate resistant acid phosphatase (TRAP) activity was detected by using an acid phosphatase kit (Sigma-Aldrich Company Ltd.)

TABLE I. Antibodies Used in This Study

Antibody	Target	Specificity	Supplier	References
FA11	Macrosialin/CD68	MΦ, DC	Serotec	Rabinowitz and Gordon [1991]
F4/80	F4/80/Emr1	Mo, MΦ, eosinophils, DC	Serotec	Hume et al. [1984]
SER4	Sialoadhesin (Sn)	MΦ	Dr. P. Crocker	Crocker et al. [1991]
5D3	Mannose receptor (MR)	MΦ, select endothelia	Serotec	Linehan et al. [1999]; Martinez-Pomares et al. [2003]
5C6	CR3/CD11b	Mo, MΦ, MNGC, OC, neutrophils and NK cells	Serotec	Rosen and Gordon [1987]
RA3-6B2	CD45R	Early Pro-B to mature B cells, some activated T-cells	BD Pharmingen	Domiati-Saad et al. [1993]
17A2	CD3 molecular complex	T-cells	BD Pharmingen	Ferrini et al. [1989]
RB6-8C5	anti-Gr-1 (Ly6G/C)	Neutrophils, Mo, MΦ, eosinophils and subset of T-cells	BD Pharmingen	Hestdal et al. [1991]
DX5	CD49b integrin α2 subunit	CD4+ T-cells, IEL, NK cells	BD Pharmingen	Arase et al. [2001]
2A11	Dectin-1	Mo, MΦ neutrophils, DC	Serotec	Taylor et al. [2002]

according to the manufacturer's instructions. For F4/80, Sn (Ser4), CR3 (5C6), macrosialin (FA11), MR (5D3), CD3, B220 (Table I) and mouse-anti-human vimentin immunohistochemistry, ABC kits were used (Vector Laboratories Ltd., Peterborough, UK) and the processing was as follows, according to the manufacturer's instructions with slight modifications: Sections were thawed and dried at 37°C for 1 h, fixed in 10% buffered formaldehyde (0.1 M PBS, pH 7.2), washed in 0.1% Triton X-100 in PBS 5 min three times, incubated at room temperature in normal serum 30 min, primary antibody 60 min, secondary antibody 30 min, ABC 30 min and in substrate DAB (peroxidase kit) for 2–5 min or 15 min in fast red (alkaline phosphatase kit). Sections were washed three times in PBS for 5 min between all steps. To inhibit the activities of endogenous enzymes, the sections were quenched in 1 mM sodium azide, 0.18% (w/v) glucose, 0.4 μl/ml glucose oxidase (Sigma-Aldrich Company Ltd.) in 0.1 M PBS (pH 7.2) at 37°C after fixation for peroxidase labelling, or pre-incubated in 50 mM levamisole (Sigma) in Tris-HCl buffer (pH 8.2) for 15 min, then reacted with AP substrate mixture with 50 mM levamisole. Sections were examined by light microscopy (Zeiss Axioplan; Carl Zeiss Ltd., Oberkochen, Germany).

For histomorphometry, the microscopic images from immunohistochemical staining were scanned by a JVC KY-F55BE 3-CCD colour video camera (Victor Company of Japan Ltd., Tokyo, Japan). At each time point (day 7, 14 and 28), six samples, three control and three with HBMF cell implantation were chosen for analysis. For total GFP-positive cell area, three sections from different levels from each mouse were scanned at a magnification 25×. To determine CR3 and F4/80 positive cell areas, at a magnification 400×, two sections from different levels and five fields per section between the tibia and anterior tibialis muscle, where sham operation or HBMF cell implantation was performed, were randomly selected. Any calcified tissue, either callus or ectopic bone was excluded from analysis to avoid interference of calcified tissue staining on determination of DAB colour. The DAB stained colour threshold was defined and the areas of all positively stained cells automatically measured using image analysis software OPTIMAS version 5.2 (Optimas Corporation, Kent, UK). The area is expressed as the area of positively stained cells within the area of imaged tissue (mm^2/mm^2).

RNA Extraction and RT-PCR

Cell and tissue samples were snap frozen in liquid nitrogen and stored at −80°C until required. Tissues were ground under liquid nitrogen using a pestle and mortar and both DNA and total RNA extracted using a Qiagen RNA/DNA kit (Qiagen, Crawley, UK) according to the manufacturer's protocol.

One microgram total RNA was used for the synthesis of cDNA. The reaction was carried out at 42°C for 50 min in a total volume of 20 μl, containing 0.5 μg oligo $(dT)_{12-18}$ primer, 1 mM each of dATP, dCTP, dGTP and dTTP, 1× first-strand buffer (50 mM Tris-HCl, 75 mM KCl, 3 mM $MgCl_2$, pH 8.3) 10 mM DTT and 200 units Superscript™ II reverse transcriptase (all from Invitrogen, Renfrew, UK). The reaction was stopped by heating to 70°C for 15 min and the volume diluted to 200 μl.

Twenty microlitres aliquots from the above mixture were used for PCR. The PCR reaction was performed in a 25 μl mix of 1× PCR buffer (20 mM Tris-HCl, 50 mM KCl, pH 8.4), 1.5 mM $MgCl_2$, 0.2 mM dNTPs, appropriate primers at 0.2 μM and 0.5 units Platinum® *Taq* DNA polymerase. Amplification reactions specific for the following cDNAs were carried out: Alkaline phosphatase (bone/liver/kidney isoform; AP), osteocalcin (OC), osteopontin (OP), collagen type I (ColI), green fluorescent protein (GFP), Cbfa1/RunX2 and glyceraldehyde phosphate dehydrogenase (GAPDH). Amplification profiles were as follows: AP—94°C for 30 s, 55°C for 30 s, 72°C for 30 s and 38 cycles; OC and OP—94°C for 30 s, 55°C for 30 s, 72°C for 30 s and 36 cycles; ColI—94°C for 30 s, 55°C for 30 s, 72°C for 30 s and 32 cycles; GFP—94°C for 30 s, 55°C for 30 s, 72°C for 1 min and 40 cycles; Cbfa1/RunX2—94°C for 30 s, 58°C for 30 s, 72°C for 30 s and 36 cycles; GAPDH—94°C for 30 s, 55°C for 30 s, 72°C for 30 s and 28 cycles. PCR products were visualised by electrophoresis in a 1% agarose gel containing ethidium bromide at 0.05 μg/ml.

Primer sequences, product sizes and GenBank numbers are listed in Table II.

Statistics

Data are presented as mean ± standard error and evaluated by Student's *t*-test in Microsoft

TABLE II. Primers for RT-PCR

Primers	Sequences	Product size (bp)	GenBank accession number	Position of primer in sequence
GAPDH	sense 5′-CGTGGAAGGACTCATGACC-3′ antisense 5′-CCAAATTCGTTGTCATACCAG-3′	446	XM_006959	585/1031
Cbfa1/RunX2	sense 5′-GCCCGTGGCCTTCAAGGTG-3′ antisense 5′-GTGCCTGCCTGGGGTCTG-3′	466	NM_001024630	618/1084
Osteocalcin	sense 5′-GCCCTCACACTCCTCGCC-3′ antisense 5′-GCCGTAGAAGCGCCGATAGG-3′	288	NM_000711	24/312
Enhanced GFP	sense 5′-GACCCTGAAGTTCATCTGCAC-3′ antisense 5′-GGCCTTGATGCCGTTCTTCTG-3′	363	AB041904	129/492

Excel. Statistical significance was set at $P < 0.05$.

RESULTS

Myeloid Markers of CB17 Scid Beige Mice

To screen innate immune cell populations, we used FACS analysis to detect myeloid cell markers (summarised in Table I) in the spleen and blood of CB17 sb mice and wild-type Balb/C mice. The results are shown in Tables III and IV and supplemental Figure 1.

There were no significant differences in the cell numbers recovered from the spleens of the two strains of mice. Among the isolated cells, the percentage of B- and T-cell numbers in CB17 sb mice was much lower ($P < 0.001$) compared with wild-type Balb/C mice, but the recovery of monocytes and red pulp macrophages was three- and five-fold higher respectively than those in wild-type Balb/C mice ($P < 0.01$ and $P < 0.05$ respectively).

FACS analysis of myeloid cell markers in peripheral blood cells of CB17 sb mice and wild-type Balb/C mice is shown in Table IV. There were no significant differences in cell numbers recovered from peripheral blood in the two strains of mice. Within the isolated cells, the percentages of B- and T-cell numbers in CB17 sb mice were lower than those in wild-type Balb/C mice ($P < 0.001$ and $P < 0.05$ respectively). The percentage of neutrophils and monocytes, however, was two- and three-fold higher respectively than in wild-type Balb/C mice ($P < 0.01$ and $P < 0.05$ respectively).

The myeloid markers in CB17 sb mice, detected using immunohistochemical techniques in the spleen, 3 weeks after sham operation or implantation of HBMF cells in the anterior tibialis muscle, are shown in Figure 1. CD68 (FA11), F4/80, sialoadhesin (Sn), mannose receptor (MR) and complement receptor 3 (CR3) are positive in spleens and in the wound area between the tibia and the anterior tibialis muscle of sham operated mice and in the anterior tibialis muscle where HBMF cells were implanted. CD3 and B220 staining was very weak in the spleen. However, positive staining of CD3 and B220 could be observed at the site of HBMF cell implantation and some weaker staining could also be seen at sham operated sites.

Elimination of Implanted HBMF Cells

The implanted HBMF cell pellets were approximately 2 mm^3 in size. In cryosections of harvested samples, implanted HBMF cells showed green eGFP fluorescence, which could be easily detected by fluorescence microscopy, and the area of human cell implantation measured using Optimas 5.0 software.

The results showed that the areas of eGFP-labelled HBMF cells declined sharply from day 7–28 after implantation (Fig. 2A).

RT-PCR of eGFP message from isolated total RNA from the tissue demonstrated the decline of eGFP expression (Fig. 2B). In parallel with the decline of eGFP expression, the levels of expression of two specific markers of osteogenic differentiation, Cbfa1 and osteocalcin, also fell dramatically from day 7–14 and were not detectable by day 28 (Fig. 2B).

After initial osteogenic differentiation followed by maintenance in αMEM containing 2% FCS in vitro with regular passaging for up to 5 months, the HBMF cells exhibited no loss of eGFP expression (Fig. 3a) and formed bone-like nodules in vitro (Fig. 3b).

Inflammatory Cell Infiltration into HBMF Cell Implanted Tissue

One week after sham operation or HBMF cell implantation, reaction callus formation was observed on the tibial surface toward the

TABLE III. FACS Analysis of Myeloid Markers in Splenocytes of Balb/C and CB17 bg Mice (unit = %, mean ± SE)

		Percentage of cells (%)							
Mouse	Cell number ($\times 10^6$)	B ($CD19^+$)	T ($CD3^+$)	NK ($CD49b^+$ $CD3^-$)	Neu ($Gr\text{-}1^{high}$)	Eos ($F4/80^+$ SSC^{high})	Mo ($F4/80^+$ $CD11b^+$)	Red Pulp MΦ ($F4/80^{high}$)	DC ($CD11c^{high}$)
Balb/c	69.9 ± 7.7	52.78 ± 0.77	25.06 ± 1.05	3.75 ± 0.03	2.26 ± 0.36	0.28 ± 0.03	2.29 ± 0.16	3.19 ± 0.19	1.60 ± 0.14
CB17 bg	34.9 ± 18.0	0.11 ± 0.03[c]	1.31 ± 0.72[c]	8.03 ± 2.03	28.05 ± 10.53	0.72 ± 0.30	8.01 ± 0.75[b]	13.22 ± 3.56[a]	2.77 ± 0.44

[a] $P < 0.05$.
[b] $P < 0.01$.
[c] $P < 0.001$.

TABLE IV. FACS Analysis of Myeloid Markers in Peripheral Blood Cells of Balb/C and CB17 bg Mice (unit = %, mean ± SE)

		Percentage of cells (%)					
Mouse	Cell number ($\times 10^6$)	B ($CD19^+$)	T ($CD3^+$)	NK ($CD49b^+$ $CD3^-$)	Neu ($Gr\text{-}1^{high}$)	Eos ($F4/80^+$ SSC^{high})	Mo ($F4/80^+$ $CD11b^+$)
Balb/c	3.89 ± 0.54	27.33 ± 1.63	26.83 ± 4.22	20.98 ± 1.15	19.89 ± 0.16	1.10 ± 0.29	6.03 ± 0.47
CB17 bg	4.71 ± 1.03	0.00 ± 0.00[c]	0.34 ± 0.17[a]	28.94 ± 2.78	43.65 ± 1.84[b]	0.75 ± 0.04	17.40 ± 2.75

[a] $P < 0.05$.
[b] $P < 0.01$.
[c] $P < 0.001$.

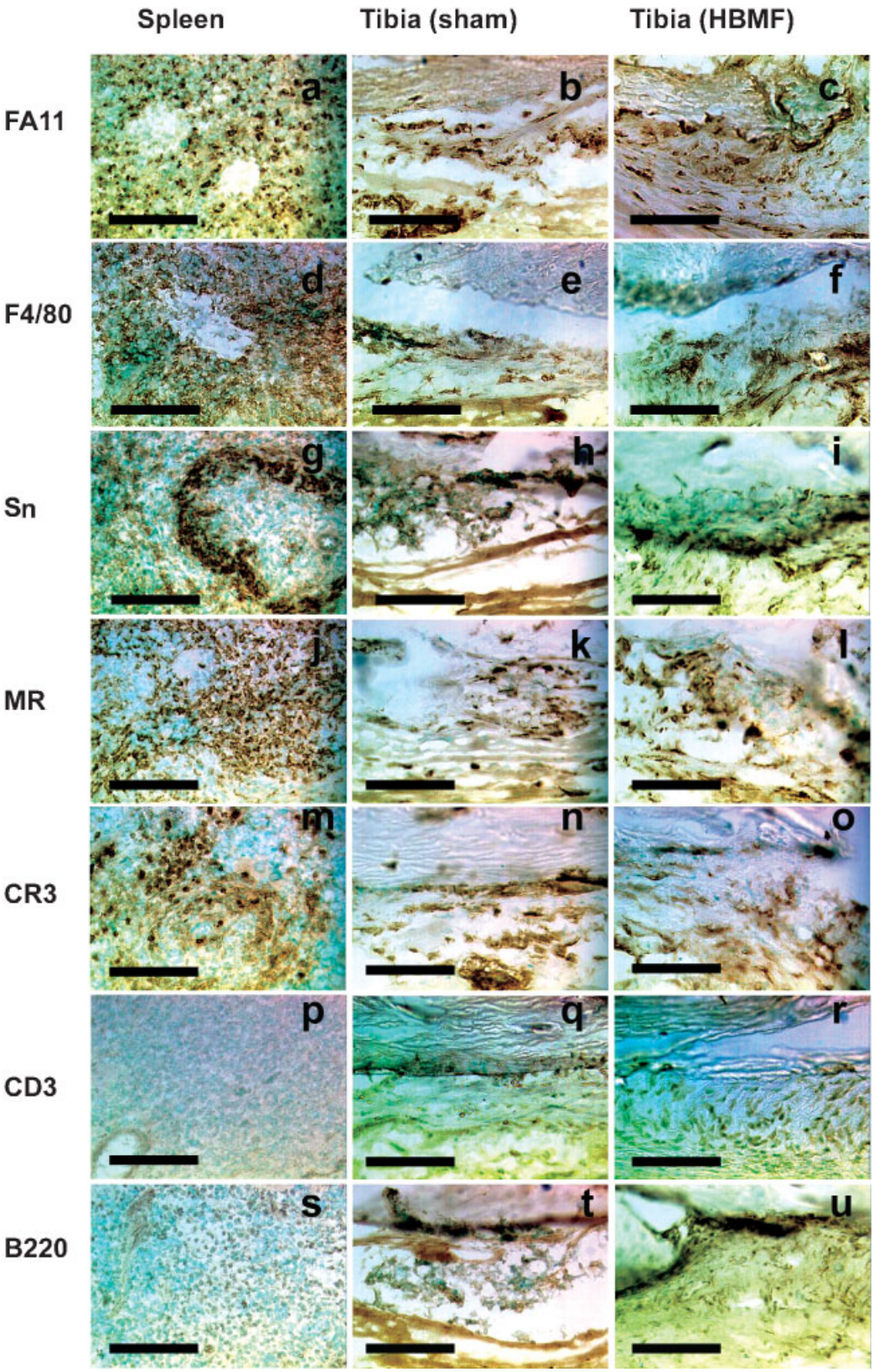

Fig. 1. Immunohistochemical detection of myeloid markers in CB17 scid beige mice, including FA11, F4/80, SN, MR, CR3(5C6), CD3 and B220 in spleens of control mice and tibia 3 weeks after sham operation (control) and HBMF cell implantation. Bar = 0.1 mm. [Color figure can be viewed in the online issue, which is available at www.interscience.wiley.com.]

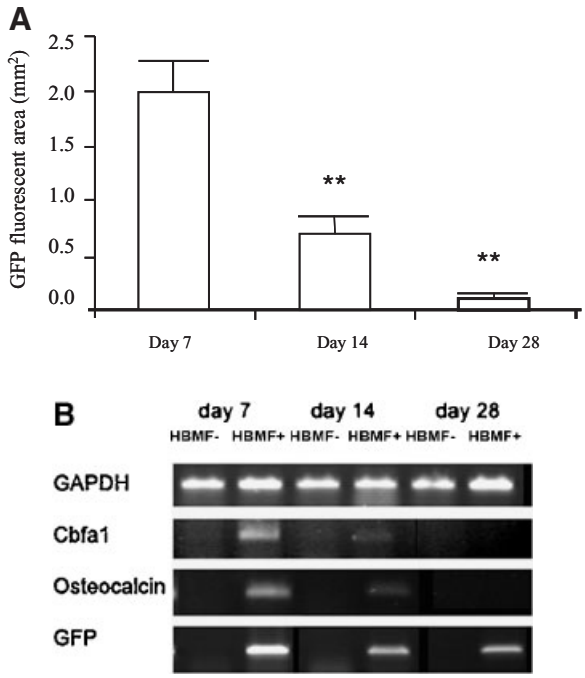

Fig. 2. Elimination of eGFP-labelled HBMF cells after implantation in CB17 scid beige mice. **A**: Histomorphometry of GFP fluorescent area in mouse anterior tibialis at 7, 14 and 28 days after HBMF cell implantation (**compared with day 7 $P < 0.01$); **B**: RT-PCR of GFP, Cbfa1 and osteocalcin (OC) at 7, 14 and 28 days after HBMF cell implantation.

wound. In HBMF cell implanted mice, there was ectopic bone formation in the anterior tibialis muscle (Fig. 3c,d). Mouse MΦ and other myeloid cells invaded tissue sites after HBMF cell implantation or sham operation over the 1–4 week time period of the experiment.

The HBMF cells in this study were genetically labelled with eGFP. Mouse MΦ and CR3-positive inflammatory cells were located by F4/80 and CR3 antibodies respectively using alkaline phosphatase as a substrate and stained using Fast Red for fluorescence microscopy (Fig. 3e,f). It was shown that F4/80 and CR3-positive cells infiltrated HBMF cell-implanted tissue and were in close contact with HBMF cells.

Using peroxidase as substrate, F4/80 and CR3-positive cells were stained brown (Supplemental Figs. 2 and 3). In control mice, MΦ and other CR3-positive inflammatory cells invaded the operation site between the tibia and the anterior tibialis muscle and formed a thin layer of inflammation (<0.1 mm). However, in the implanted mice, HBMF cells and invading mouse cells formed a broader gap between the tibia and the anterior tibialis muscle. MΦ and CR3-positive cells were widely distributed in this region. There were more MΦ and CR3-positive cells around the ectopic, mineralised bone and on the surface of the callus than in non-calcified tissues.

Image analysis software, Optimas 5.2, was used to capture the area of brown colouration of the stained cells by using a threshold setting and the areas over this threshold quantified. The average area of F4/80 and CR3-positive cell regions over background of non-calcified tissue (mm^2/mm^2), is shown in Figure 4A,B. The average area of F4/80 positive cells in HBMF cell implanted samples was 0.080 mm^2/mm^2 at 1 week, 0.078 mm^2/mm^2 at 2 weeks and declined to 0.035 mm^2/mm^2 at 4 weeks. By contrast, in sham-operated mice, the areas were 0.024 mm^2/mm^2, 0.010 mm^2/mm^2 and 0.0003 mm^2/mm^2, which represents 29.75%, 12.42% and 9.83% at weeks 1, 2 and 4 respectively of the values seen in the HBMF cells implanted samples ($P < 0.01$) (Fig. 4A).

The average areas of CR3 positive cells in the sham and HBMF cell implanted mice showed the same trend as with F4/80. However, the areas in the sham-operated samples were 30.97%, 23.02% and 25.62% of those observed in the groups implanted with HBMF cells at weeks 1, 2 and 4 respectively, and these values were statistically significant ($P < 0.01$) (Fig. 4B). This demonstrates that even in the absence of T- and B-cells, xenografts of HBMF cells still induced strong inflammatory responses in immunocompromised mice. The areas of F4/80 and CR3 positive cells within HBMF cell-implanted samples were also compared and showed that F4/80 was only 73.89% and 66.61% of CR3 at 1 and 2 weeks respectively. However, this was reversed at 4 weeks, as F4/80 staining was 17.63% greater than CR3-staining at this time point.

Remodelling of Mineralised Tissue by Macrophage-Lineage Cells

Multinuclear giant cells (MNGCs) appeared on the surface of calcified tissue at the surgical site as early as 5 days after operation. In the control group, there was very little ectopic calcification and the MNGCs existed mainly on the surface of the bone and reactive callus. The positive staining of tartrate-resistant acid phosphatase (TRAP) (Fig. 5a) and cell morphology demonstrated that they resembled activated

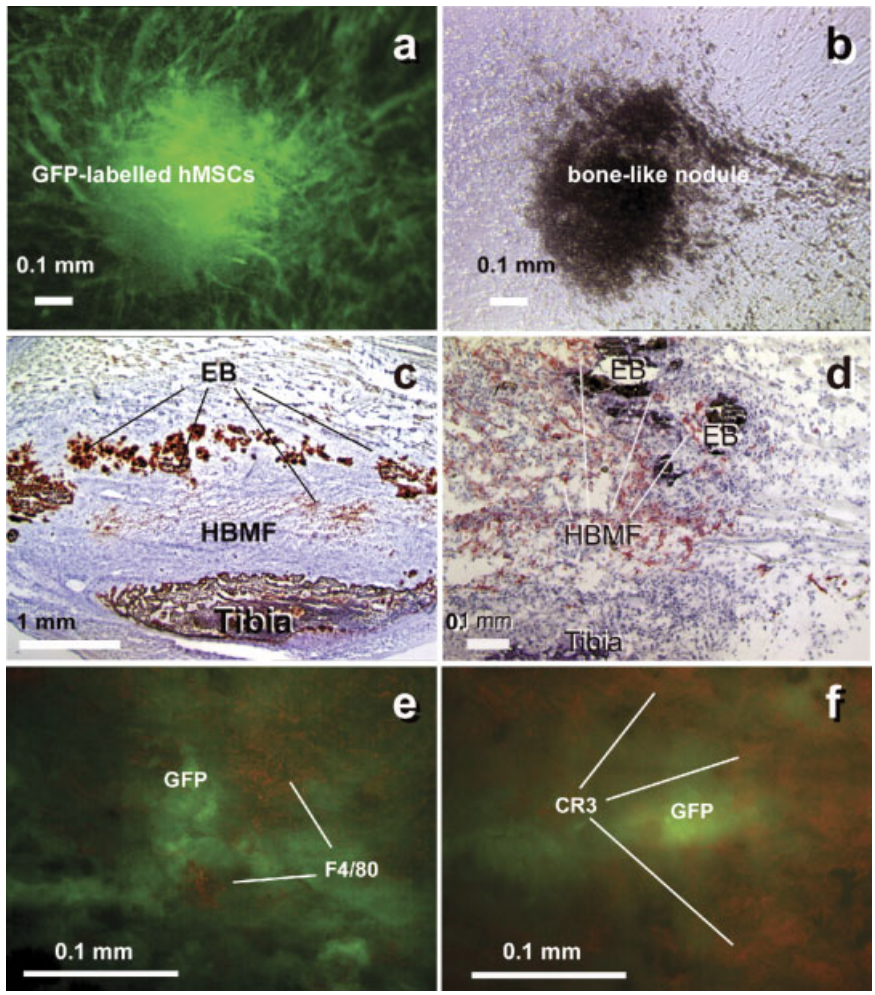

Fig. 3. Micrographs of EGFP-labelled HBMF in vitro and after implantation in vivo in CB17 sb mice after implantation. **a**: GFP-labelled HBMF cells after extended (5 months) culture with multiple passages in vitro by fluorescence microscopy 28 days after plating. **b**: The same field as (a) by light microscopy showing bone-like nodules formed by GFP-labelled HBMF cells. **c**: Ectopic bone formation by implanted HBMF cells. EB, ectopic bone-like matrix formation. HBMF, location of site of HBMF implantation between muscle and tibia. **d**: High power magnification of ectopic bone formation. EB, ectopic bone-like matrix. HBMFs were stained as red by a mouse-anti-human vimentin antibody. These cells are not only on the surface but also embedded in mineralised bone-like matrix. **e**: F4/80 staining for macrophages; GFP, eGFP-labelled HBMF cells; F4/80, F4/80-stained cells, (**f**), CR3(5C6) staining of inflammatory cells; GFP, eGFP-labelled HBMF cells; CR3, CR3-stained cells. Bar = 0.1 mm. [Color figure can be viewed in the online issue, which is available at www.interscience.wiley.com.]

osteoclasts involved in callus resorption and bone remodelling. These cells were also CR3-positive and negative for F4/80 (Fig. 5c,e).

The implanted HBMF cells formed mineralised tissue, which either integrated into the reactive callus that formed close to the tibia or ossified as ectopic bone near the tibialis muscle. In the callus, MNGCs reacted similarly to those seen in the control group. However, in the ectopic bone tissue, mineralised tissue was almost fully covered by MNGCs. These cells were TRAP-positive indicating that they were potentially bone-resorbing cells (Fig. 5b). However, both F4/80 and CR3-positive staining marked their monocyte-macrophage origin (Fig. 5d,f).

It was observed that the callus that formed in both the sham-operated controls and HBMF cell-implanted mice was remodelled and that the ectopic bone formed in the HBMF cell-implanted mice was completely eliminated by 4 weeks.

DISCUSSION

Natural host defence against foreign challenge is mediated by the phylogenetically older

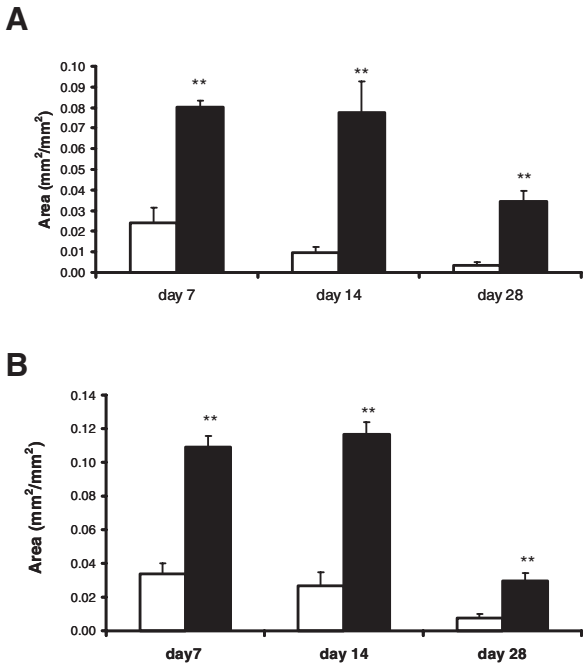

Fig. 4. Histomorphometry of F4/80 and CR3 positive cell areas observed at the site of HBMF implantation. **A**: Histomorphometry of F4/80 positive cell area, $^{**}P < 0.01$; **B**: Histomorphometry of CR3(5C6) positive cell area, $^{**}P < 0.01$.

innate immune system [Hoffmann et al., 1999; Kimbrell and Beutler, 2001] whereas the adaptive immune system, dominated by B- and T-lymphocytes has arisen only relatively recently [Kimbrell and Beutler, 2001].

The host defence to xenografts is poorly understood; in particular after xenotransplantation in immunodeficient mice where adaptive immune responses are not functional. Depletion and/or genetic manipulation studies have shown that B-cells, IL-4, IL-5 and eosinophils, IFN-γ, Fc receptors, NK cells and perforin are by themselves not essential for xenograft rejection [Fox et al., 2001]. Macrophages are the dominant infiltrating cells in xenografts undergoing rejection; however, T-cells are required for macrophages to act as direct effectors of xenograft rejection [Fox et al., 2001]. In the absence of T-cells, as in SCID mice, macrophages and other innate immune cells do not have immediate effects on xenografts; however, their long-term effects are largely unknown. Our study reveals that xenografts of HBMF cells into CB17 sb mice are slowly eliminated. The majority of implanted HBMF cells are eliminated within 4 weeks, although in some previous experiments in our laboratory we have observed some cell survival up to 10 weeks after implantation [Xia et al., 2004]. Part of this elimination is likely to be because of natural bone remodelling and dependent on lack of mechanical requirement for the bone formed. In any event, components of the innate immune system are clearly demonstrated to be intimately involved in elimination of the developed tissues.

To understand the nature of the immune system in CB17 sb mice, we studied the impact of their deficiencies on the numbers of innate immune cells, such as monocytes (Mo), macrophages (MΦ), neutrophils (N_{eu}), eosinophils (E_{os}) and NK cells in tissues and peripheral blood, using novel and established myeloid markers, including Dectin-1, CD11b, F4/80 and Gr-1 (Table I), as previously described [Taylor et al., 2003]. In addition to flow-cytometric analysis, various antibodies recognising murine myeloid antigens, in particular those used to detect macrophages such as FA11 [Rabinowitz and Gordon, 1991], Sn [Crocker et al., 1991] and MR [Linehan et al., 1999; Martinez-Pomares et al., 2003], were also employed to identify the cellular distribution in tissue by immunohistochemistry.

As expected CB17 sb mice lack B- and T-cells, however, compared to wild type mice we observed increases in some myeloid cell populations, such as Mo and MΦ in spleen and N_{eu} in blood. The overrepresentation of Mo, MΦ and N_{eu} is most likely a consequence of the deficiency in the adaptive immune system. Even though there is a functional NK cell deficiency in beige background mice, no significant difference in NK cell numbers was observed between the CB17 sb and wild-type Balb/C.

Significant immunostaining for CR3 (CD11b/CD18) and F4/80 after HBMF cell implantation into CB17 sb mice demonstrated substantial infiltration of innate immune cells. CD11b is highly expressed on many myeloid cells, such as Mo, N_{eu}, E_{os}, subsets of MΦ, NK cells [Rosen and Gordon, 1987], some dendritic cells (DC) [Shortman and Liu, 2002] and subsets of lymphocytes. F4/80 is one of the best-characterised MΦ markers present on most tissue MΦ [Hume et al., 1984], but also expressed by E_{os} and some DC. The immunohistochemical staining of CR3 and F4/80 highlights the presence of myeloid cells, in particular macrophages, that are recruited to the site of HBMF cell implantation.

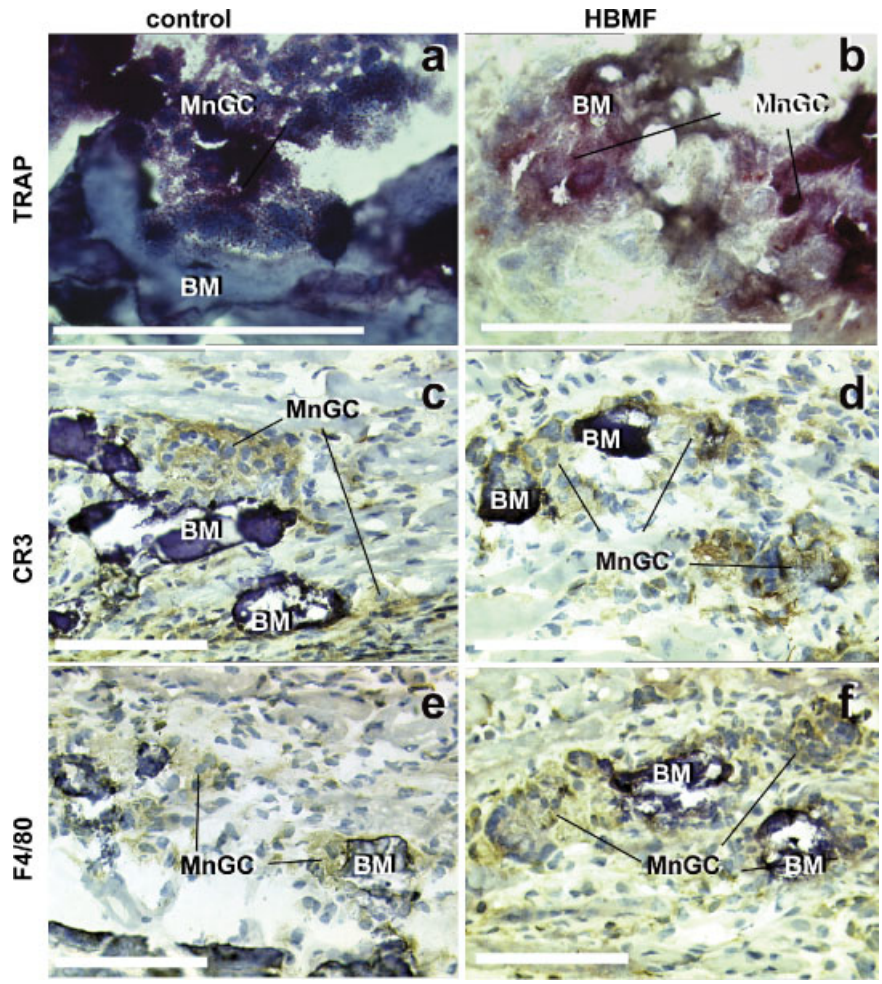

Fig. 5. Resorption of callus and ectopic mineralised bone matrix (BM) by osteoclasts (OC) and multinuclear giant cells (MNGC). **a**: TRAP staining of OC in tibia callus resorption, sham-operated control group; **b**: TRAP staining of MNGC in ectopic BM in HBMF cell implanted group; **c**: CR3-positive OC in callus resorption, control group; **d**: CR3-positive MNGCs in ectopic BM resorption in HBMF cell implanted group; **e**: F4/80-negative OC in callus resorption, control group; **f**: F4/80-positive MNGC in ectopic BM resorption in HBMF cells implanted group. Bar = 0.1 mm. [Color figure can be viewed in the online issue, which is available at www.interscience.wiley.com.]

In experimental models of transplantation, there is no evidence of pathogenic infection suggesting that innate immune activation can be triggered by non-infectious stimuli [He et al., 2003]. Stress proteins such as heat shock protein 60 and fibronectin have been identified as non-infectious stimuli of innate signalling via Toll-like receptor [Aderem and Ulevitch, 2000] or other pathways [Bouchon et al., 2001]. Antigen-independent stimuli including ischaemia, reperfusion, surgical injury or systemic stress may also contribute to the initiation of an inflammatory response [He et al., 2003]. There is no direct evidence for a mechanism of activation of macrophages and other innate immune cells in the current study. However, the elimination of implanted HBMF cells implies that without functional B- and T-cells, the remaining innate immune system in immunocompromised mice can still react against human cell xenotransplantation. As a secreting cell the activated macrophage produces a wide spectrum of cytokines that may promote an unfavourable environment for human cell survival, differentiation and function.

An interesting phenomenon in this study is the clearance of the mineralised matrix by the host. The osteoclast is a tissue specific macrophage-like polykaryon created by the differentiation of monocyte/macrophage precursor cells

at or near the bone surface [Boyle et al., 2003] and it is believed to be the only cell specialised in bone resorption [Athanasou, 1996]. However, it has proved difficult to distinguish osteoclasts from other cells, particularly multinucleated giant cells resulting from macrophage fusion [Athanasou, 1996]. Not only can monocytes/macrophages resorb bone matrix, but also monocyte and macrophage populations, derived from many sources and at various stages of maturation, can be induced to differentiate into osteoclasts [Teitelbaum, 2000]. In our study, the multinuclear cells on the surface of bone and callus resorption in control and HBMF cell implanted mice were tartrate-resistant acid phosphatase (TRAP) positive, but F4/80 negative. This suggests that they are osteoclasts as osteoclasts lack F4/80 expression [Hume et al., 1984]. The cells eroding mineralised bone matrix formed by implanted HBMF cells were also multinuclear and TRAP positive; however, these cells expressed both CR3 and F4/80. In the current study, we do not have sufficient evidence to identify these cells as fused macrophages, and they may represent osteoclasts at early stages of differentiation.

The criteria to distinguish if these cells are macrophages or osteoclasts, such as ruffled borders, clear zones, the ability to form resorption lacunae on a bone substrate and to respond to calcitonin in vitro [Athanasou, 1996], have not been used in the current study. Nevertheless, these cells effectively erode the ectopic mineralised matrix and also remove the embedded osteogenic cells, which differentiated from implanted HBMF cells.

We conclude that CB17 sb mice retain functional components of the innate immune system, which effectively responds to HBMF xenotransplantation. Even though this response does not result in direct killing of implanted HBMF cells, the elicited inflammatory cells may lead to slow elimination of implanted HBMF cells and the matrix formed by differentiated human cells. This study highlights the importance of innate immune cells in the anti-xenograft response and suggests that strategies to block the activities of these cells may ameliorate the progressive long-term elimination of xenotransplants. Also the value of porous cell carriers, such as calcium phosphate ceramics or collagen sponges that are known to be suitable for conductive or inductive bone formation with extended cell survival, may reside partly in generation of a protective environment during the generation of the tissue.

ACKNOWLEDGMENTS

We thank Kyri Mitrophanous and Fiona Ellard (Oxford Biomedica Plc., Oxford) for supplying retroviral vectors for HBMF cell labelling, Nick Athanasou for supplying samples for HBMF cell isolation and comments on discussion of multinuclear giant cells, and Elizabeth Darley for advice and help with immunohistochemistry.

REFERENCES

Aderem A, Ulevitch RJ. 2000. Toll-like receptors in the induction of the innate immune response. Nature 406:782–787.

Arase H, Saito T, Phillips JH, Lanier LL. 2001. Cutting edge: The mouse NK cell-associated antigen recognized by DX5 monoclonal antibody is CD49b (alpha 2 integrin, very late antigen-2). J Immunol 167:1141–1144.

Arinzeh TL, Peter SJ, Archambault MP, van den Bos C, Gordon S, Kraus K, Smith A, Kadiyala S. 2003. Allogeneic mesenchymal stem cells regenerate bone in a critical-sized canine segmental defect. J Bone Joint Surg Am 85(A):1927–1935.

Athanasou NA. 1996. Cellular biology of bone-resorbing cells. J Bone Joint Surg Am 78:1096–1112.

Bouchon A, Facchetti F, Weigand MA, Colonna M. 2001. TREM-1 amplifies inflammation and is a crucial mediator of septic shock. Nature 410:1103–1107.

Boyle WJ, Simonet WS, Lacey DL. 2003. Osteoclast differentiation and activation. Nature 423:337–342.

Boynton E, Aubin J, Gross A, Hozumi N, Sandhu J. 1996. Human osteoblasts survive and deposit new bone when human bone is implanted in SCID mouse. Bone 18:321–326.

Caplan AI. 1994. The mesengenic process. Clin Plast Surg 21:429–435.

Cilloni D, Carlo-Stella C, Falzetti F, Sammarelli G, Regazzi E, Colla S, Rizzoli V, Aversa F, Martelli MF, Tabilio A. 2000. Limited engraftment capacity of bone marrow-derived mesenchymal cells following T-cell-depleted hematopoietic stem cell transplantation. Blood 96: 3637–3643.

Crocker PR, Kelm S, Dubois C, Martin B, McWilliam AS, Shotton DM, Paulson JC, Gordon S. 1991. Purification and properties of sialoadhesin, a sialic acid-binding receptor of murine tissue macrophages. EMBO J 10:1661–1669.

Domiati-Saad R, Ogle EW, Justement LB. 1993. Administration of anti-CD45 mAb specific for a B cell-restricted epitope abrogates the B cell response to a T-dependent antigen *in vivo*. J Immunol 151:5936–5947.

Ferrini S, Prigione I, Bottino C, Ciccone E, Tambussi G, Mammoliti S, Moretta L, Moretta A. 1989. Monoclonal antibodies which react with the T cell receptor gamma/delta recognize different subsets of CD3 + WT31- T lymphocytes. Eur J Immunol 19:57–61.

Fox A, Harrison LC. 2000. Innate immunity and graft rejection. Immunol Rev 173:141–147.

Fox A, Mountford J, Braakhuis A, Harrison LC. 2001. Innate and adaptive immune responses to nonvascular xenografts: Evidence that macrophages are direct effectors of xenograft rejection. J Immunol 166:2133–2140.

Friedenstein AJ, Chailakhjan RK, Lalykina KS. 1970. The development of fibroblast colonies in monolayer cultures of guinea-pig bone marrow and spleen cells. Cell Tissue Kinet 3:393–403.

Froidevaux S, Loor F. 1991. A quick procedure for identifying doubly homozygous immunodeficient scid beige mice. J Immunol Methods 137:275–279.

Gotherstrom C, Ringden O, Westgren M, Tammik C, Le Blanc K. 2003. Immunomodulatory effects of human foetal liver-derived mesenchymal stem cells. Bone Marrow Transplant 32:265–272.

Gronthos S, Zannettino AC, Hay SJ, Shi S, Graves SE, Kortesidis A, Simmons PJ. 2003. Molecular and cellular characterisation of highly purified stromal stem cells derived from human bone marrow. J Cell Sci 116:1827–1835.

Gundle R, Joyner CJ, Triffitt JT. 1995. Human bone tissue formation in diffusion chamber culture *in vivo* by bone-derived cells and marrow stromal fibroblastic cells. Bone 16:597–601.

He H, Stone JR, Perkins DL. 2003. Analysis of differential immune responses induced by innate and adaptive immunity following transplantation. Immunology 109: 185–196.

Hestdal K, Ruscetti FW, Ihle JN, Jacobsen SE, Dubois CM, Kopp WC, Longo DL, Keller JR. 1991. Characterization and regulation of RB6-8C5 antigen expression on murine bone marrow cells. J Immunol 147:22–28.

Hoffmann JA, Kafatos FC, Janeway CA, Ezekowitz RA. 1999. Phylogenetic perspectives in innate immunity. Science 284:1313–1318.

Hume DA, Loutit JF, Gordon S. 1984. The mononuclear phagocyte system of the mouse defined by immunohistochemical localization of antigen F4/80: Macrophages of bone and associated connective tissue. J Cell Sci 66:189–194.

Kimbrell DA, Beutler B. 2001. The evolution and genetics of innate immunity. Nat Rev Genet 2:256–267.

Koc ON, Peters C, Aubourg P, Raghavan S, Dyhouse S, DeGasperi R, Kolodny EH, Yoseph YB, Gerson SL, Lazarus HM, Caplan AI, Watkins PA, Krivit W. 1999. Bone marrow-derived mesenchymal stem cells remain host-derived despite successful hematopoietic engraftment after allogeneic transplantation in patients with lysosomal and peroxisomal storage diseases. Exp Hematol 27:1675–1681.

Le Blanc K, Rasmusson I, Sundberg B, Gotherstrom C, Hassan M, Uzunel M, Ringden O. 2004. Treatment of severe acute graft-versus-host disease with third party haploidentical mesenchymal stem cells. Lancet 363: 1439–1441.

Lee K, Majumdar MK, Buyaner D, Hendricks JK, Pittenger MF, Mosca JD. 2001. Human mesenchymal stem cells maintain transgene expression during expansion and differentiation. Mol Ther 3:857–866.

Lee JJ, Nam CE, Kook H, Maciejewski JP, Kim YK, Chung IJ, Park KS, Lee IK, Hwang TJ, Kim HJ. 2003. Constitution and telomere dynamics of bone marrow stromal cells in patients undergoing allogeneic bone marrow transplantation. Bone Marrow Transplant 32:947–952.

Liechty KW, MacKenzie TC, Shaaban AF, Radu A, Moseley AM, Deans R, Marshak DR, Flake AW. 2000. Human mesenchymal stem cells engraft and demonstrate site-specific differentiation after in utero transplantation in sheep. Nat Med 6:1282–1286.

Linehan SA, Martinez-Pomares L, Stahl PD, Gordon S. 1999. Mannose receptor and its putative ligands in normal murine lymphoid and nonlymphoid organs: In situ expression of mannose receptor by selected macrophages, endothelial cells, perivascular microglia, and mesangial cells, but not dendritic cells. J Exp Med 189:1961–1972.

Martinez-Pomares L, Reid DM, Brown GD, Taylor PR, Stillion RJ, Linehan SA, Zamze S, Gordon S, Wong SY. 2003. Analysis of mannose receptor regulation by IL-4, IL-10, and proteolytic processing using novel monoclonal antibodies. J Leukoc Biol 73:604–613.

Matsumoto S, Shibuya I, Kusakari S, Segawa K, Uyama T, Shimada A, Umezawa A. 2005. Membranous osteogenesis system modeled with KUSA-A1 mature osteoblasts. Biochim Biophys Acta 1725:57–63.

Niyibizi C, Wang S, Mi Z, Robbins PD. 2004. The fate of mesenchymal stem cells transplanted into immunocompetent neonatal mice: Implications for skeletal gene therapy via stem cells. Mol Ther 9:955–963.

Oreffo RO, Kusec V, Romberg S, Triffitt JT. 1999. Human bone marrow osteoprogenitors express estrogen receptor-alpha and bone morphogenetic proteins 2 and 4 mRNA during osteoblastic differentiation. J Cell Biochem 75:382–392.

Owen M. 1988. Marrow stromal stem cells. J Cell Sci Suppl 10:63–76.

Pittenger MF, Mackay AM, Beck SC, Jaiswal RK, Douglas R, Mosca JD, Moorman MA, Simonetti DW, Craig S, Marshak DR. 1999. Multilineage potential of adult human mesenchymal stem cells. Science 284: 143–147.

Platt JL. 1999. Prospects for xenotransplantation. Pediatr Transplant 3:193–200.

Rabinowitz SS, Gordon S. 1991. Macrosialin, a macrophage-restricted membrane sialoprotein differentially glycosylated in response to inflammatory stimuli. J Exp Med 174:827–836.

Rosen H, Gordon S. 1987. Monoclonal antibody to the murine type 3 complement receptor inhibits adhesion of myelomonocytic cells *in vitro* and inflammatory cell recruitment *in vivo*. J Exp Med 166:1685–1701.

Schuler W, Weiler IJ, Schuler A, Phillips RA, Rosenberg N, Mak TW, Kearney JF, Perry RP, Bosma MJ. 1986. Rearrangement of antigen receptor genes is defective in mice with severe combined immune deficiency. Cell 46:963–972.

Shortman K, Liu YJ. 2002. Mouse and human dendritic cell subtypes. Nat Rev Immunol 2:151–161.

Taylor PR, Brown GD, Reid DM, Willment JA, Martinez-Pomares L, Gordon S, Wong SY. 2002. The beta-glucan receptor, dectin-1, is predominantly expressed on the surface of cells of the monocyte/macrophage and neutrophil lineages. J Immunol 169:3876–3882.

Taylor PR, Brown GD, Geldhof AB, Martinez-Pomares L, Gordon S. 2003. Pattern recognition receptors and

differentiation antigens define murine myeloid cell heterogeneity ex vivo. Eur J Immunol 33:2090–2097.

Teitelbaum SL. 2000. Bone resorption by osteoclasts. Science 289:1504–1508.

Toma C, Pittenger MF, Cahill KS, Byrne BJ, Kessler PD. 2002. Human mesenchymal stem cells differentiate to a cardiomyocyte phenotype in the adult murine heart. Circulation 105:93–98.

Triffitt JT, Oreffo RO, Virdi AS, Xia Z. 2001. Osteogenic stem-cell characterization and development: Potentials for cytotherapy. Cytotherapy 3:413–416.

Tsuda H, Wada T, Ito Y, Uchida H, Dehari H, Nakamura K, Sasaki K, Kobune M, Yamashita T, Hamada H. 2003. Efficient BMP2 gene transfer and bone formation of mesenchymal stem cells by a fiber-mutant adenoviral vector. Mol Ther 7:354–365.

Xia Z, Ye H, Choong C, Ferguson DJ, Platt N, Cui Z, Triffitt JT. 2004. Macrophagic response to human mesenchymal stem cell and poly(epsilon-caprolactone) implantation in nonobese diabetic/severe combined immunodeficient mice. J Biomed Mater Res 71A:538–548.

Xia Z, Ye H, Locklin RM, Ferguson DJ, Cui Z, Triffitt JT. 2005. Efficient characterisation of human cell-bioceramic interactions *in vitro* and *in vivo* by using enhanced GFP-labelled mesenchymal stem cells. Biomaterials 26:5790–5800.

Yamamoto T, Ecarot B, Glorieux FH. 1991. *In vivo* osteogenic activity of isolated human bone cells. J Bone Miner Res 6:45–51.